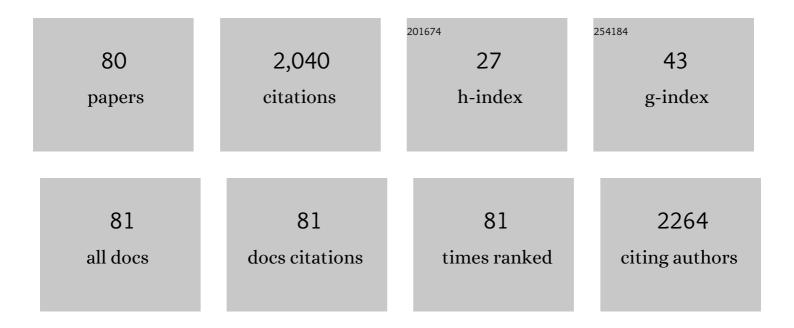


List of Publications by Year in descending order

Source: https://exaly.com/author-pdf/717913/publications.pdf Version: 2024-02-01



SHENC

#	Article	IF	CITATIONS
1	Graphene-synergized 2D covalent organic framework for adsorption: A mutual promotion strategy to achieve stabilization and functionalization simultaneously. Journal of Hazardous Materials, 2018, 358, 273-285.	12.4	121
2	A Designed ZnO@ZIFâ€8 Core–Shell Nanorod Film as a Gas Sensor with Excellent Selectivity for H ₂ over CO. Chemistry - A European Journal, 2017, 23, 7969-7975.	3.3	103
3	Facile Fabrication of Mn ₂ O ₃ Nanoparticle-Assembled Hierarchical Hollow Spheres and Their Sensing for Hydrogen Peroxide. ACS Applied Materials & Interfaces, 2015, 7, 9526-9533.	8.0	88
4	Synthesis of Microporous Covalent Phosphazene-Based Frameworks for Selective Separation of Uranium in Highly Acidic Media Based on Size-Matching Effect. ACS Applied Materials & Interfaces, 2018, 10, 28936-28947.	8.0	84
5	A flexible zinc tetrazolate framework exhibiting breathing behaviour on xenon adsorption and selective adsorption of xenon over other noble gases. Journal of Materials Chemistry A, 2015, 3, 10747-10752.	10.3	80
6	Control of pore chemistry in metal-organic frameworks for selective uranium extraction from seawater. Microporous and Mesoporous Materials, 2019, 288, 109567.	4.4	80
7	Immobilization of uranium by biomaterial stabilized FeS nanoparticles: Effects of stabilizer and enrichment mechanism. Journal of Hazardous Materials, 2016, 302, 1-9.	12.4	79
8	Polypropylene Modified with Amidoxime/Carboxyl Groups in Separating Uranium(VI) from Thorium(IV) in Aqueous Solutions. ACS Sustainable Chemistry and Engineering, 2017, 5, 1924-1930.	6.7	75
9	Polymer brushes on graphene oxide for efficient adsorption of heavy metal ions from water. Journal of Applied Polymer Science, 2019, 136, 48156.	2.6	74
10	Nano-TiO ₂ Imparts Amidoximated Wool Fibers with Good Antibacterial Activity and Adsorption Capacity for Uranium(VI) Recovery. Industrial & Engineering Chemistry Research, 2018, 57, 1826-1833.	3.7	73
11	MOF-SMO hybrids as a H2S sensor with superior sensitivity and selectivity. Sensors and Actuators B: Chemical, 2019, 292, 32-39.	7.8	67
12	Aggregation-induced emission active tetraphenylethene-based sensor for uranyl ion detection. Journal of Hazardous Materials, 2016, 318, 363-370.	12.4	54
13	Highly Efficient Recovery of Uranium from Seawater Using an Electrochemical Approach. Industrial & Engineering Chemistry Research, 2018, 57, 8078-8084.	3.7	53
14	Pt–Ir binary hydrophobic catalysts: Effects of Ir content and particle size on catalytic performance for liquid phase catalytic exchange. International Journal of Hydrogen Energy, 2009, 34, 8723-8732.	7.1	49
15	Fluorescent recognition of uranyl ions by a phosphorylated cyclic peptide. Chemical Communications, 2015, 51, 11769-11772.	4.1	49
16	Metal–organic framework derived nanoporous carbons with highly selective adsorption and separation of xenon. Journal of Materials Chemistry A, 2018, 6, 13696-13704.	10.3	49
17	Phosphate-Functionalized Polyethylene with High Adsorption of Uranium(VI). ACS Omega, 2017, 2, 3267-3275.	3.5	46
18	Adsorption behavior of uranium on polyvinyl alcohol-g-amidoxime: Physicochemical properties, kinetic and thermodynamic aspects. Science China Chemistry, 2013, 56, 1495-1503.	8.2	37

SHENG

#	Article	IF	CITATIONS
19	Fluorescent BINOL-based sensor for thorium recognition and a density functional theory investigation. Journal of Hazardous Materials, 2013, 263, 638-642.	12.4	35
20	Mass spectrometry for the determination of fission products 135Cs, 137Cs and 90Sr: A review of methodology and applications. Spectrochimica Acta, Part B: Atomic Spectroscopy, 2016, 119, 65-75.	2.9	35
21	Functional polymer brushes for highly efficient extraction of uranium from seawater. Journal of Materials Science, 2019, 54, 3572-3585.	3.7	35
22	Development and application of mass spectrometric techniques for ultra-trace determination of 236U in environmental samples-A review. Analytica Chimica Acta, 2017, 995, 1-20.	5.4	34
23	Efficient capture of actinides from strong acidic solution by hafnium phosphonate frameworks with excellent acid resistance and radiolytic stability. Chemical Engineering Journal, 2019, 355, 159-169.	12.7	33
24	Fluorogenic Thorium Sensors Based on 2,6â€Pyridinedicarboxylic Acid‣ubstituted Tetraphenylethenes with Aggregationâ€Induced Emission Characteristics. Chemistry - an Asian Journal, 2016, 11, 49-53.	3.3	32
25	Recovery of uranium(VI) from aqueous solution by amidoxime functionalized wool fibers. Journal of Radioanalytical and Nuclear Chemistry, 2016, 307, 1471-1479.	1.5	31
26	Selective separation of thorium from rare earths and uranium in acidic solutions by phosphorodiamidate-functionalized silica. Chemical Engineering Journal, 2020, 392, 123717.	12.7	31
27	Hydrophobic Pt catalysts with different carbon substrates for the interphase hydrogen isotope separation. Separation and Purification Technology, 2011, 77, 214-219.	7.9	27
28	Polyamidoxime functionalized with phosphate groups by plasma technique for effective U(VI) adsorption. Journal of Industrial and Engineering Chemistry, 2018, 67, 380-387.	5.8	27
29	Preparation and characterization of hydrophobic Pt–Fe catalysts with enhanced catalytic activities for interface hydrogen isotope separation. Journal of Hazardous Materials, 2012, 209-210, 478-483.	12.4	26
30	Polyvinyl alcohol fibers with functional phosphonic acid group: synthesis and adsorption of uranyl (VI) ions in aqueous solutions. Journal of Radioanalytical and Nuclear Chemistry, 2013, 296, 1331-1340.	1.5	26
31	Enhanced xenon adsorption and separation with an anionic indium–organic framework by ion exchange with Co ²⁺ . RSC Advances, 2017, 7, 55012-55019.	3.6	26
32	Zero valent iron/poly(amidoxime) adsorbent for the separation and reduction of U(<scp>vi</scp>). RSC Advances, 2016, 6, 52076-52081.	3.6	24
33	The preparation of organophosphorus ligand-modified SBA-15 for effective adsorption of Congo red and Reactive red 2. RSC Advances, 2019, 9, 13476-13485.	3.6	23
34	Ultra-trace determination of the ¹³⁵ Cs/ ¹³⁷ Cs isotopic ratio by thermal ionization mass spectrometry with application to Fukushima marine sediment samples. Journal of Analytical Atomic Spectrometry, 2019, 34, 301-309.	3.0	22
35	The roles of metals and their oxide species in hydrophobic Pt–Ru catalysts for the interphase H/D isotope separation. International Journal of Hydrogen Energy, 2010, 35, 10118-10126.	7.1	21
36	A uranium capture strategy based on self-assembly in a hydroxyl-functionalized ionic liquid extraction system. Chemical Communications, 2019, 55, 6894-6897.	4.1	20

SHEN

#	Article	IF	CITATIONS
37	Density functional theory study of the Eu(III) and Am(III) complexes with two 1,10-phenanthroline-type ligands. Polyhedron, 2015, 95, 86-90.	2.2	19
38	Preparation of ZnO nanoparticle loaded amidoximated wool fibers as a promising antibiofouling adsorbent for uranium(<scp>vi</scp>) recovery. RSC Advances, 2019, 9, 18406-18414.	3.6	19
39	Novel polyazamacrocyclic receptor impregnated macroporous polymeric resins for highly efficient capture of palladium from nitric acid media. Separation and Purification Technology, 2020, 233, 115953.	7.9	19
40	"One-pot―synthesis of amidoxime via Pd-catalyzed cyanation and amidoximation. Organic and Biomolecular Chemistry, 2015, 13, 2541-2545.	2.8	17
41	Density functional theory investigations on the binding modes of amidoximes with uranyl ions. Dalton Transactions, 2016, 45, 3120-3129.	3.3	16
42	Highly selective extraction of uranium from wastewater using amine-bridged diacetamide-functionalized silica. Journal of Hazardous Materials, 2022, 435, 129022.	12.4	15
43	Exploring the ability of triple quadrupole inductively coupled plasma mass spectrometry for the determination of Pu isotopes in environmental samples. Journal of Analytical Atomic Spectrometry, 2021, 36, 2330-2337.	3.0	13
44	Enhanced electro-mechanical actuation strain in polyaniline nanorods/silicone rubber nanodielectric elastomer films. Applied Physics Letters, 2014, 104, 242903.	3.3	11
45	Chemical treatments on the cuticle layer enhancing the uranium(VI) uptake from aqueous solution by amidoximated wool fibers. Journal of Radioanalytical and Nuclear Chemistry, 2017, 314, 1927-1937.	1.5	11
46	An initial demonstration of hierarchically porous niobium alkylphosphonates coordination polymers as potent radioanalytical separation materials. Journal of Chromatography A, 2017, 1504, 35-45.	3.7	10
47	In-situ deposited ZnO film-based sensor with controlled microstructure and exposed facet for high H2 sensitivity. Journal of Alloys and Compounds, 2017, 704, 117-123.	5.5	9
48	Carboxylate functionalized wool fibers for removal of Cu(II) and Pb(II) from aqueous solution. Desalination and Water Treatment, 2016, 57, 17367-17376.	1.0	8
49	Pd atalyzed Vinylation of Aryl Halides with Inexpensive Organosilicon Reagents Under Mild Conditions. Chemistry - A European Journal, 2018, 24, 10324-10328.	3.3	8
50	Efficient Synthesis of 1,5-Disubstituted Carbohydrazones Using K2CO3 As a Carbonyl Donor. Organic Letters, 2014, 16, 2398-2401.	4.6	7
51	Trace impurity analysis in uranium materials by rapid separation and ICP-MS/MS measurement with matrix matched external calibration. Microchemical Journal, 2021, 169, 106615.	4.5	7
52	Automated method for concurrent determination of thorium (²³⁰ Th, ²³² Th) and uranium (²³⁴ U, ²³⁵ U, ²³⁸ U) isotopes in water matrices with ICP-MS/MS. Journal of Analytical Atomic Spectrometry, 2022, 37, 919-928.	3.0	7
53	Promising density functional theory methods for predicting the structures of uranyl complexes. RSC Advances, 2014, 4, 50261-50270.	3.6	6
54	Embedded atom model for the liquid U–10Zr alloy based on density functional theory calculations. RSC Advances, 2015, 5, 61495-61501.	3.6	6

SHEN

#	Article	IF	CITATIONS
55	Stereocontrolled C(sp3)–P bond formation with non-activated alkyl halides and tosylates. RSC Advances, 2017, 7, 24652-24656.	3.6	6
56	Complexation of U(VI) with picolinic acid in aqueous solution at variable temperatures: Potentiometric, spectrophotometric and calorimetric studies. Journal of Chemical Thermodynamics, 2017, 113, 350-357.	2.0	6
57	Determination of trace rare earth elements in uranium ore samples by triple quadrupole inductively coupled plasma mass spectrometry. Journal of Analytical Atomic Spectrometry, 2021, 36, 2144-2152.	3.0	6
58	Complexation behavior of Eu(III), Tb(III), Tm(III), and Am(III) with three 1,10-phenanthroline-type ligands: insights from density functional theory. Journal of Molecular Modeling, 2015, 21, 185.	1.8	5
59	More than ten percent ionization efficiency for Tc measurement by negative thermal ionization mass spectrometry. Journal of Analytical Atomic Spectrometry, 2019, 34, 2229-2235.	3.0	5
60	A base-mediated three-component coupling reaction for the synthesis of phosphorohydrazones. Tetrahedron, 2013, 69, 10068-10072.	1.9	4
61	High performance of amidoxime/amine functionalized polypropylene for uranyl (VI) from aqueous solution. E-Polymers, 2013, 13, .	3.0	4
62	The Hydrolytic Stability and Degradation Mechanism of a Hierarchically Porous Metal Alkylphosphonate Framework. Nanomaterials, 2018, 8, 166.	4.1	4
63	Cerium separation with NaBiO ₃ nanoflower material <i>via</i> an oxidation adsorption strategy. Journal of Materials Chemistry A, 2020, 8, 7907-7913.	10.3	4
64	Density functional study of uranyl (VI) amidoxime complexes. Chinese Physics B, 2012, 21, 093102.	1.4	3
65	Simulation of irradiation uniformity for polyethylene and polypropylene in various high energy fields. Radiation Physics and Chemistry, 2018, 151, 47-52.	2.8	3
66	Improvement of hydrogen isotope exchange reactions on Li4SiO4 ceramic pebble by catalytic metals. Chinese Chemical Letters, 2012, 23, 936-940.	9.0	2
67	Hot-corrosion behavior of Ti ₃ SiC ₂ in a eutectic mixture of LiCl–KCl salts in air. RSC Advances, 2015, 5, 21629-21633.	3.6	2
68	Density Function Theory Study on the Reaction Mechanism of Cerium with Oxygen for Ce-bearing Aerosol Particle Formation. Journal Wuhan University of Technology, Materials Science Edition, 2020, 35, 501-505.	1.0	2
69	Energetics of gaseous and volatile fission products in molten U–10Zr alloy: A density functional theory study. Journal of Nuclear Materials, 2015, 466, 583-587.	2.7	1
70	Capillary electrophoresis coupled with inâ€column fiberâ€optic laserâ€induced fluorescence detection for the rapid separation of neodymium. Electrophoresis, 2016, 37, 2657-2662.	2.4	1
71	Density Functional Theory Investigations on the Mechanism of Formation of Pa(V) Ion in Hydrous Solutions. Molecules, 2019, 24, 1169.	3.8	1
72	Density functional theory investigations on the coordination of Pa(v) with N,N-dialkylamide. New Journal of Chemistry, 2020, 44, 9477-9484.	2.8	1

SHEN

#	Article	IF	CITATIONS
73	Preparation and Catalytic Activity of Pt Based Hydrophobic Catalysts Adulterated with Fe Series Elements. Wuji Cailiao Xuebao/Journal of Inorganic Materials, 2011, 26, 91-96.	1.3	1
74	Removal of hexavalent chromium ions from aqueous solution by amidoxime functionalized wool fibers. , 0, 58, 137-143.		1
75	A simple method for Ce–Nd separation using nano-NaBiO3: Application in the isotopic analysis of U, Sr, Pb, Nd, and Hf in uranium ores. Talanta, 2022, 245, 123443.	5.5	1
76	Investigating the performance of a Rh metal catalyst in hydrogen–deuterium exchange reactions in methane for application in low-temperature membrane separators. Fusion Engineering and Design, 2014, 89, 2666-2671.	1.9	0
77	Complexation of a macrocyclic ligand, 2,6-di (N-methyl)formamide-calix[4]pyridine, with Eu(III) and extraction of Eu(III) and Am(III). Radiochimica Acta, 2018, 106, 301-310.	1.2	Ο
78	Theoretical simulation for the chemico-physical properties of α-quartz and stishovite Si1-Ce O2 via first-principles. Physica B: Condensed Matter, 2020, 582, 411906.	2.7	0
79	The formation mechanism of cerium-bearing aerosols with the aid of chemical explosions in airtight scenarios. New Journal of Chemistry, 2021, 45, 20696-20712.	2.8	Ο
80	Influence of Carrier on Catalytic Activity of Platinum Based Hydrophobic Catalysts. Wuji Cailiao Xuebao/Journal of Inorganic Materials, 2010, 25, 279-284.	1.3	0